Title

Normal human mammary epithelial cells spontaneously escape senescence and acquire genomic changes

Journal

Nature, 409(6820)

ISSN

0028-0836

Authors

Romanov, Serguei R
Kozakiewicz, B Krystyna
Holst, Charles R
et al.

Publication Date

2001-02-01

DOI

10.1038/35054579

Peer reviewed

23. Lee, L. *et al.* Positioning of the mitotic spindle by a cortical-microtubule capture mechanism. *Science* **287,** 2260–2262 (2000).
24. Korinek, W. S., Copeland, M. J., Chaudhuri, A. & Chant, J. Molecular linkage underlying microtubule orientation toward cortical sites in Yeast. *Science* **287,** 2257–2259 (2000).
25. Rose, L. S. & Kemphues, K. The let-99 gene is required for proper spindle orientation during cleavage of the *C. elegans* embryo. *Development* **125,** 1337–1346 (1998).
26. Brenner, S. The genetics of *Caenorhabditis elegans*. *Genetics* **77,** 71–94 (1974).
27. Morton, D. G., Roos, J. M. & Kemphues, K. J. *par-4*, a gene required for cytoplasmic localisation and determination of specific cell types in *Caenorhabditis elegans* embryogenesis. *Genetics* **130,** 771–790 (1992).
28. Gönczy, P. *et al.* Dissection of cell division processes in the one cell stage *Caenorhabditis elegans* embryo by mutational analysis. *J. Cell Biol.* **144,** 927–946 (1999).
29. Raich, W. B., Moran, A. N., Rothman, J. H. & Hardin, J. Cytokinesis and midzone microtubule organization in *Caenorhabditis elegans* require the kinesin-like protein ZEN-4. *Mol. Biol. Cell* **9,** 2037–2049 (1998).
30. Powers, J., Bossinger, O., Rose, D., Strome, S. & Saxton, W. A nematode kinesin required for cleavage furrow advancement. *Curr. Biol.* **8,** 1133–1136 (1998).

Supplementary information (including QuickTime movies corresponding to Figs 2 and 4) is available on *Nature's* World-Wide Web site (http://www.nature.com).

Acknowledgements

We thank K. Kemphues for mutants *it71* and *it5*; K. Oegema for experimental assistance; A. Desai, E.-L. Florin and E. Hannak for discussions; R. Pepperkok, K. Schütze and R. Schütze for supplying the laser microdissection setup; and T. Bouwmeester, A. Desai, E. Hannak, E. Karsenti, F. Nédélec and K. Oegema for help with improving the manuscript.

Correspondence and requests for materials should be addressed to A.H. (e-mail: hyman@embl-heidelberg.de).

Normal human mammary epithelial cells spontaneously escape senescence and acquire genomic changes

Serguei R. Romanov*, B. Krystyna Kozakiewicz*, Charles R. Holst*, Martha R. Stampfer†, Larisa M. Haupt* & Thea D. Tlsty*

** Department of Pathology and UCSF Comprehensive Cancer Center, University of California at San Francisco, San Francisco, California 94143-0506, USA*
† Lawrence Berkeley National Laboratory, Berkeley, California 94720, USA

Senescence and genomic integrity are thought to be important barriers in the development of malignant lesions[1]. Human fibroblasts undergo a limited number of cell divisions before entering an irreversible arrest, called senescence[2]. Here we show that human mammary epithelial cells (HMECs) do not conform to this paradigm of senescence. In contrast to fibroblasts, HMECs exhibit an initial growth phase that is followed by a transient growth plateau (termed selection or M0; refs 3–5), from which proliferative cells emerge to undergo further population doublings (~20–70), before entering a second growth plateau (previously termed senescence or M1; refs 4–6). We find that the first growth plateau exhibits characteristics of senescence but is not an insurmountable barrier to further growth. HMECs emerge from senescence, exhibit eroding telomeric sequences and ultimately enter telomere-based crisis to generate the types of chromosomal abnormalities seen in the earliest lesions of breast cancer. Growth past senescent barriers may be a pivotal event in the earliest steps of carcinogenesis, providing many genetic changes that predicate oncogenic evolution. The differences between epithelial cells and fibroblasts provide new insights into the mechanistic basis of neoplastic transformation.

To analyse cell-specific differences in growth and senescence, we characterized the *in vitro* proliferation barriers in isogenic HMECs and human mammary fibroblasts (HMFs) from healthy individuals[3,7,8]. Similar to previous studies in human skin fibroblasts[1] and HMECs[3–5,9], both the epithelial and fibroblast cell populations underwent a limited number of population doublings before entering a plateau (Fig. 1, HMF phase b, HMEC phase b). This plateau in fibroblasts has been variously termed the Hayflick limit[2], irreversible replicative senescence, and mortality stage 1 (M1)[1]). The cells enlarged in size, flattened in shape, became vacuolated (Fig. 1), and expressed senescence-associated β-galactosidase[10] (SA-β-gal; data not shown).

Low incorporation of bromodeoxyuridine (BrdU) and minimal presence of MCM2 protein, a DNA replication licensing factor[26], indicated a low proliferative index. In addition, Annexin-V staining indicated a low death index (data not shown). Further characterization showed that human foreskin fibroblasts, pre-selection HMECs and HMFs each (1) maintained genomic integrity (Fig. 2; ref. 8); (2) maintained intact cell-cycle checkpoint control (data not shown); (3) exhibited a 2N to 4N DNA content ratio of ≈ 4 at phase b (Table 1); and (4) had mean telomere restriction fragment (TRF) lengths that were similar at senescence (Fig. 3). By the morphological, behavioural and molecular criteria described above, HMFs and HMECs senesce in a manner similar to human skin fibroblasts[1]. 'M0' of HMECs thus corresponds to 'M1' of fibroblasts.

The ability of HMECs and HMFs to spontaneously overcome senescence differs by several orders of magnitude. In skin fibroblasts, senescence can last for years (at least 3 yr; T.D.T., unpublished data), cells remain viable if fed routinely[11], and the frequency of

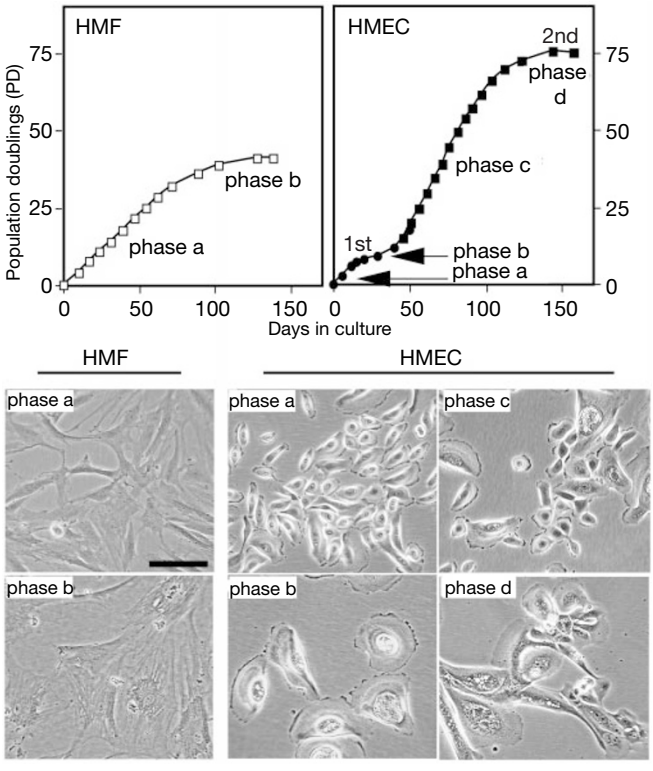

Figure 1 HMF and HMEC growth curves and cell morphologies *in vitro*. Tissue was dissociated with collagenase and hyaluronidase, and plated in parallel cultures: one in medium (DMEM) that supported the growth of fibroblasts and the other in medium (MEGM) that supported the growth of epithelial cells. The growth curve and microscopic morphology of both mammary fibroblast and epithelial cells from donor 48 during the first phase of logarithmic growth (phase a), and the first growth plateau (phase b) are shown for each population. The second epithelial phase of proliferation (phase c) and the second epithelial growth plateau (phase d) are also shown. Scale bar, 100 μm.

spontaneous emergence is $< 10^{-9}$ (data not shown; and ref. 12). Similarly, HMFs failed to produce proliferating cells from senescent populations even after 5 months in continuous culture in either serum-containing or serum-free media ($< 6 \times 10^{-7}$; data not shown). In contrast to fibroblasts and consistent with previous reports[3,5], HMECs maintained at the first plateau in serum-free media sporadically emerge at a high frequency and generate clusters of small, refractile cells (Fig. 1, HMEC phase c; $1.43 \pm 0.04 \times 10^{-4}$ (donor 48, mean ± s.d., $n = 4$) and $1 \pm 1 \times 10^{-5}$(donor 184, $n = 4$)). Pre- and post-selection HMECs showed typical heterogeneous expression of cytokeratins when examined by immuno-cytochemistry (data not shown; and ref. 13). As reported previously, HMECs that emerge from the first plateau (phase b in Fig. 1) lose expression of the p16 protein (see Supplementary Information; and refs 5, 9, 14).

After a second period of exponential growth (Fig. 1, HMEC phase c), HMECs entered a second growth plateau (Fig. 1, HMEC phase d). Unexpectedly, this plateau was critically different from the senescent, arrested state despite the fact that they both showed SA-β-gal staining (data not shown). The cells at the second plateau displayed many hallmarks of cell crisis. HMECs at this stage were heterogeneous in size and morphology (Fig. 1, HMEC phase d). More importantly, they continued to incorporate BrdU ($16.3 \pm 1.1\%$, 4-h pulse, $n = 2$) and retained high levels of MCM2 protein (> 50% of nuclei strongly staining for MCM2; data not shown). On FACS analysis, the 2N to 4N DNA ratio was roughly 1 (data not shown), typical of a population of cells in crisis[1,27]. This high proliferative index was counterbalanced by an increase in cell death. A significant fraction (~20%) of epithelial cells at the second plateau stained with Annexin-V, an indicator of cell death. In contrast, < 1% of isogenic senescent HMFs or HMECs at the first plateau were Annexin-V positive. Although DNA fragmentation characteristic of apoptosis was not detectable by TUNEL (terminal deoxyribonucleotide transferase (TdT)-mediated dUTP nick end labelling) assay, we did observe significant fragmentation of nuclei (micronucleation) in these cells as documented by DNA staining of interphase nuclei (data not shown). Thus, HMECs at the second plateau were fundamentally different from HMECs at the first plateau or fibroblast cells at senescence. They exhibited many of the characteristics of viral oncoprotein-induced crisis, with an

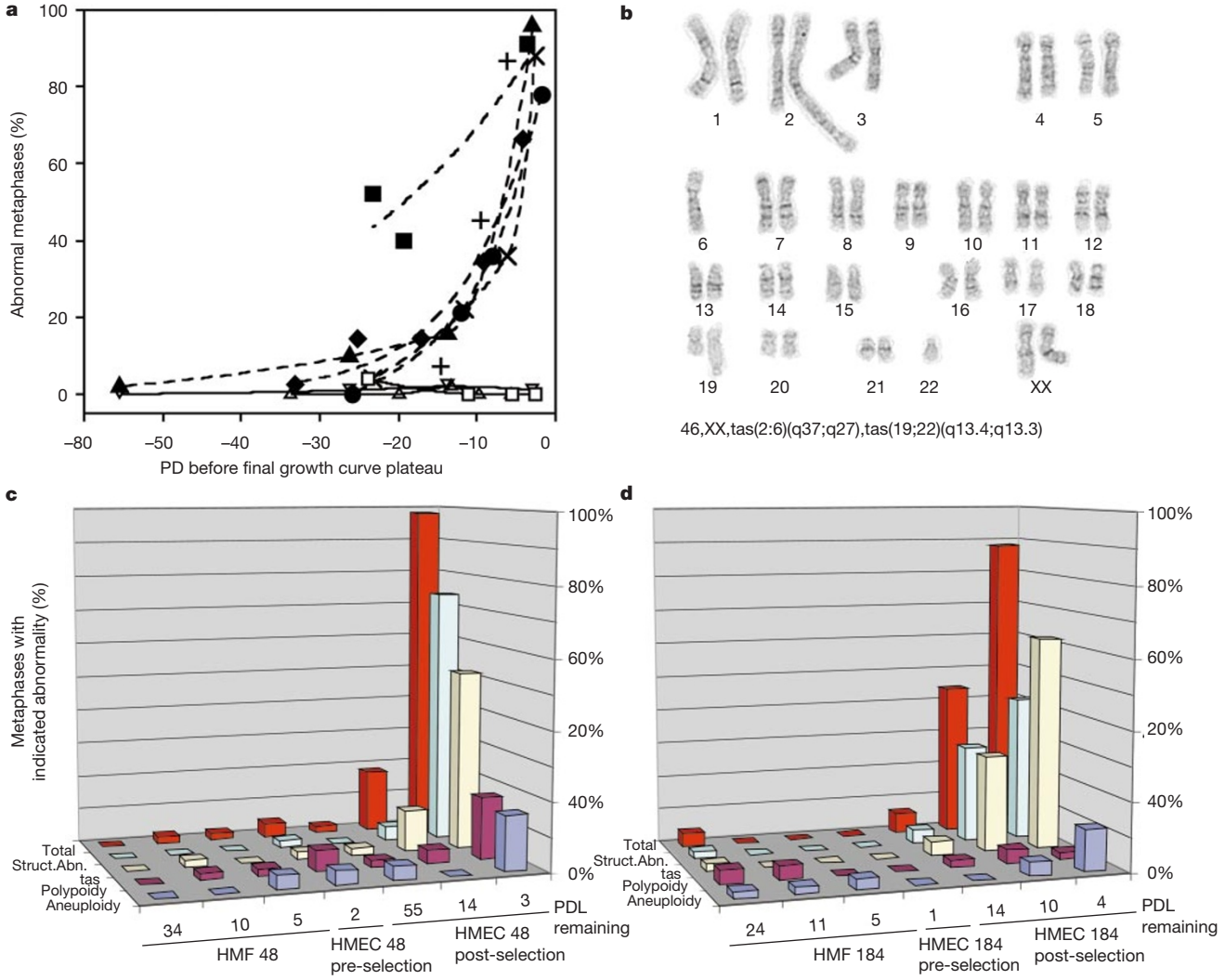

Figure 2 Spontaneous genomic instability in human mammary epithelial cells. **a**, Kinetics of accumulation of karyotypic abnormalities. The percentages of metaphase spreads with structural chromosomal abnormalities were determined as a function of the number of population doublings (PD) before final growth plateaus (0 PD). HMF populations: 48 (open triangles) and 184 (open squares). Human skin fibroblasts (open inverted triangles). HMEC populations: 48 (filled triangles), 184 spiral K (filled squares), 184 birdie ('+'), 4678-2 ('×'), 1001-3 (filled circles) and 4144-1 (filled diamonds). **b**, Representative abnormal karyotype from HMEC 48. **c**, **d**, Types of chromosomal abnormalities observed in HMEC 48 and 184, respectively. Definitions: Total, all structural abnormalities and telomeric associations, not including numerical abnormalities; Struct. Abn., deletions, duplications, rings, marker chromosomes, chromatid exchanges and translocations; tas, telomeric associations; polyploidy, multiples of a diploid chromosome complement; aneuploidy, additions or deletions of whole chromosomes.

important exception that no immortalized variants have yet been detected.

Cytogenetic analysis of post-selection HMECs at selected passages (Fig. 1, HMEC phase c) showed that gross chromosomal abnormalities appeared in virtually every metaphase spread as the cells approached the second growth plateau (Fig. 2). In all cases, including several HMEC populations obtained commercially, the abnormalities accumulated rapidly, beginning between 10 and 20 population doublings before the final passage of cells (Fig. 2a), and coincided with slowing of the proliferation rates. In these cells, both the per cent of abnormal metaphases and the number of abnormalities per metaphase increased. The abnormalities included translocations, deletions, other rearrangements, telomeric associations, polyploidy and aneuploidy (Fig. 2b–d). Substantial polyploidy (~25%) was detected by flow analysis at final passages of post-senescent HMECs (data not shown). Microscopy revealed anaphase bridges and failed cytokineses (data not shown). The accumulation of chromosomal abnormalities was independent of donor age (range 16–50 yr) and total proliferative potential of epithelial populations (range 30–60 population doublings).

The timing and spectrum of chromosomal abnormalities, especially the numerous telomeric associations, suggested that late-passage HMECs had entered a state similar to telomere-based crisis[16]. Therefore, various aspects of telomere metabolism were assessed in serial subcultures of HMECs and HMFs. Both cell populations lacked telomerase activity (data not shown; and ref. 17) and exhibited a similar rate of telomere erosion (about 30 base pairs (bp) per population doubling; data not shown). As mentioned above, mean TRF lengths in isogenic HMECs at the first growth plateau and HMF at senescence were equivalent and similar to that in the earliest available passage of post-selection HMECs. Further proliferation of the post-selection HMECs was accompanied by continued shortening of the telomeres (Fig. 3a) down to a broad range of mean TRF lengths (~3.5 kb) at the second plateau. Length distribution of telomeres at each plateau was also assessed by quantitative analysis of fluorescence *in situ* hybridization (Q-FISH) of telomeric repeats[15] (Fig. 3b–d). Consistent with the above determination of mean TRF lengths, mean fluorescence intensity at individual telomeres was diminished significantly (> 55%) in HMECs at the second plateau as compared with those at the first plateau (Fig. 3c, d). In addition, the average number of telomeres with no signal per metaphase spread was ~4 and ~2 in senescent fibroblasts and epithelial cells at the first plateau, respectively, and increased to ~18 in epithelial cells at the second plateau. Thus, the HMECs that emerged from senescence ultimately entered a telomere-based crisis-like state.

There are striking parallels between late-generation telomerase-deficient p53 mutant mice and late-passage post-selection HMECs. In wild-type mice, the activation of p53 mediates response to telomere dysfunction[18], leading to p21 induction and cell-cycle arrest[19,20]. Cells from the p53-mutant mice, like the post-selection HMECs, lack telomerase activity, and lack the p53-dependent arrest induced by critically shortened or dysfunctional telomeres. In both cell populations, these conditions generate similar types of chromosomal abnormalities. However, HMECs only attain this state on silencing p16 and emerging from senescence.

We assessed p53, its modulator $p14^{ARF}$ and a downstream effector, p21, in serial subcultures of HMFs and HMECs (see Supplementary Information). Consistent with previous reports of these proteins in human skin fibroblasts[21,22], as HMFs grew to senescence they exhibited minimal changes in total p53 protein levels, a modest increase followed by a slight decrease of p21 protein expression, and an increase in p16 protein levels. Similar expression was seen in HMECs at the first growth plateau. c-Myc protein did not change during epithelial cell culture.

Contrary to expectations, we observed an increase in total p53 protein levels in HMECs on their emergence from senescence but not on induction of senescence (phase b) or at the second plateau (phase d). An increase in $p14^{ARF}$ and p21, and a decrease in p16 accompanied this upregulation of p53. Both p53 and p21 proteins showed nuclear localization in post-selection cells (data not shown). Although most post-selection HMEC populations retained a constant level of p53 protein through the second plateau, only one sample (donor 48) showed further elevation of p53 protein that was not accompanied by further increases in $p14^{ARF}$ or p21 (see Supplementary Information). These data suggest that, as HMECs emerge from senescence, unidentified signals activate the p53 pathway but fail to explain why these post-selection cells can proliferate in the presence of elevated p53 and p21.

These studies have several important ramifications. First, they challenge traditional views of how and when cells acquire genomic changes in cancer by providing a cell-intrinsic mechanism that, early in the neoplastic process, generates several simultaneous genetic changes without obligatory exposure to physical, viral or chemical mutagenic agents. Second, although post-selection HMECs have commonly been regarded as normal[4,5], the present observations refute this assumption. These cells do not express p16, they lack proper checkpoint control[7] and they do not maintain genomic integrity (Fig. 2). Third, these findings redefine a high frequency spontaneous event that occurs in HMECs and show that 'M0', and not 'M1', is actually senescence. HMECs spontaneously emerge from senescence, whereas isogenic fibroblasts do not. Should these cells arise *in vivo* (a proposal consistent with preliminary observations), they would provide generative material for human carcinogenesis. Therefore, our observations that HMEC proliferation beyond senescence leads to telomeric dysfunction,

Table 1 Summary of human cell characteristics at different growth plateaux

	Fibroblasts		Mammary epithelial cells		
Characteristic	Senescence	Crisis*	1st plateau	2nd plateau	Crisis*
Lack of increase in cell number	+	+	+	+	+
SA-β-gal staining	+	+	+	+	+
BrdU incorporation	–	+	–	+	+
Cell death	–	+	–	+	+
Genomic instability	–	+	–	+	+
2N/4N ratio	>4	~1	>4	~1	?
Polyploidy	low	high	low	high	?
MCM2 expresion	low	high	low	high	?
Population expansion beyond growth plateau	–	+	+	?	+
Existing nomenclature	Hayflick limit, Senescence, Irreversible replicative senescence M1	Crisis, Apparent, proliferative arrest M2	Selection, Senescence, Terminal arrest M0	Senescence, Replicative senescence M1	Crisis M2
Proposed nomenclature	Senescence	Crisis	Selection	Agonescence	Crisis

*These properties describe viral oncoprotein-induced crisis.
‡See ref. 28.

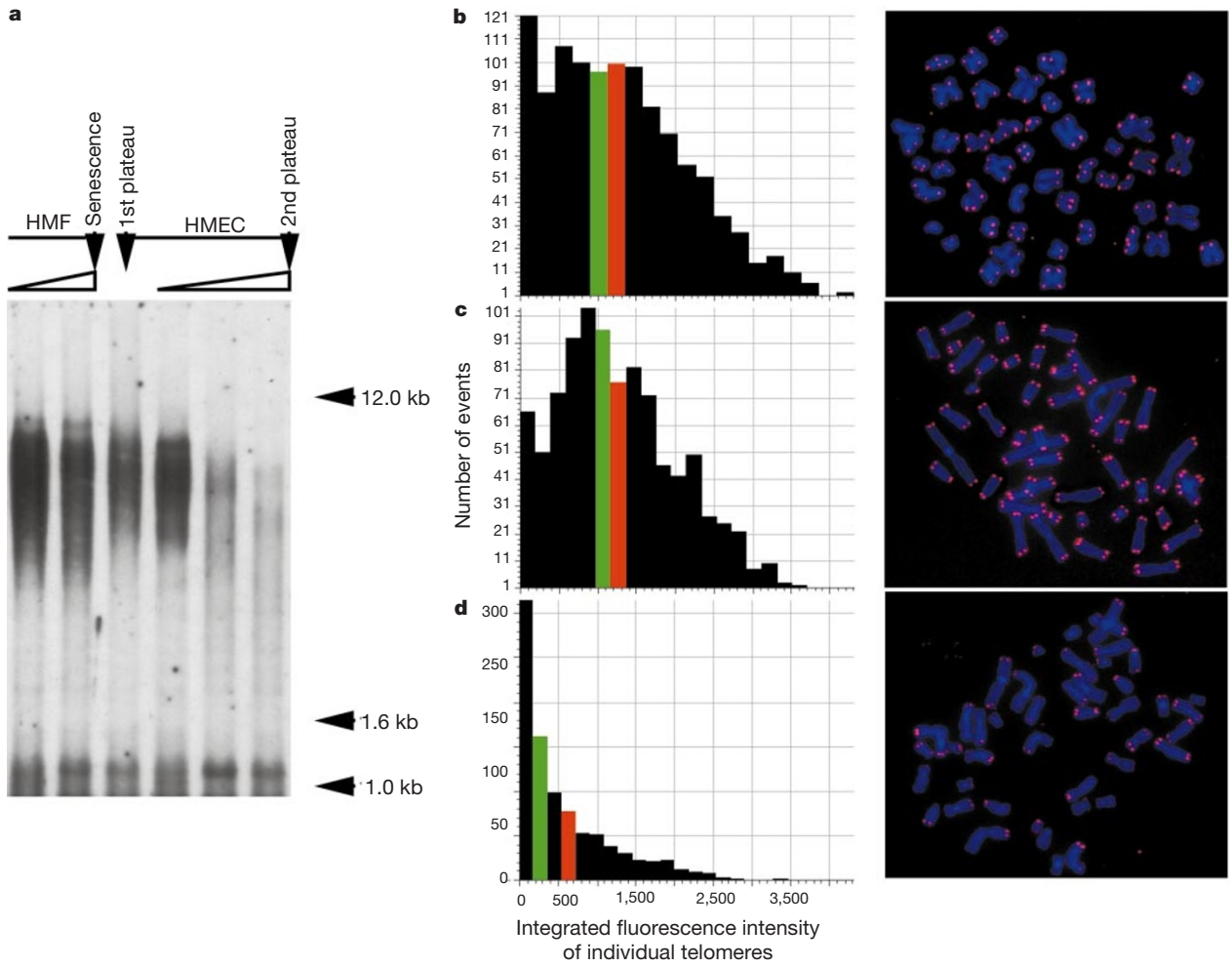

Figure 3 Post-selection HMECs continue to shorten telomeres beyond the length detected in senescent HMFs and HMECs at the first growth plateau. **a**, TRF analysis of HMF 48 (75 PD), senescent HMF 48 (42 PD), pre-selection HMEC 48 at first growth plateau (12 PD), and post-selection HMEC 48 at 20 PD, 65 PD and at second growth plateau (75 PD). **b**–**d**, Quantitative FISH analysis of telomeric repeats in senescent HMF 48 (**b**), HMEC 48 cells at first growth plateau (**c**) and HMEC 48 cells at second growth plateau (**d**). Shown are representative images of *in situ* hybridization of Cy3-$(C_3TA_2)_3$ PNA probe (red) to metaphase chromosomes (blue) and histograms of distribution of integrated fluorescence intensities of $>1{,}000$ individual telomeres. Red and green bars indicate the position of mean and median values, respectively, for each data set.

coupled with observations that telomeric dysfunction leads to carcinogenesis in mice[19,20], might explain the early steps in carcinogenesis.

Finally, these observations identify clinical opportunities. They provide potential markers for assessing susceptibility to neoplastic transformation in individuals as well as potential targets for prevention and therapy. Several markers (Table 1; and Supplementary Information) clearly identify the different cellular states and may allow the identification of these cells *in vivo*. Remarkably, the earliest lesions in breast cancer, hyperplasias, show abnormally controlled proliferation but relatively few chromosomal structural abnormalities[23]—a phenotype similar to early passage post-selection HMECs. The more progressed lesions in breast cancer, DCIS (ductal carcinoma *in situ*), also show the types of chromosomal aberrations observed in late-passage HMECs[24]. We propose that these properties of HMECs *in vitro* are critically relevant to their transformation processes *in vivo*. Agents that minimize HMEC transition past the growth plateaux should decrease the incidence of breast cancer. Given that irreversible senescence and tight control of genomic stability are believed to be important barriers for the development of cancerous lesions, our observations also suggest that there is a much higher risk of neoplastic transformation originating in mammary epithelial tissue than in mesenchymal tissue, a prediction consistent with extensive epidemiological studies[25]. □

Methods

Cells and cell culture

Isolation of isogenic sets of human breast epithelial cells and fibroblasts (that is, from the same gland) has been described[3]. Briefly, tissue from reduction mammoplasty was digested to epithelial organoids and the accompanying fibroblasts. Cells from donors 48 and 184 were obtained from a 16-year-old and a 21-year-old woman, respectively, and showed no pathologic epithelial cells. We grew and subcultured epithelial cells using two different media: MM, which contains 0.5% fetal bovine serum and several growth factors, and MEGM, a serum-free medium containing growth factors and bovine pituitary extract (BioWittaker, USA). Cell doubling times were 18–24 h in either medium. Three additional populations of human breast epithelial cells, all derived from reduction mammoplasty (1001-3, 4144-2 and 4678-2) were purchased from BioWhittaker. Fibroblasts were grown in DMEM with 10% fetal calf serum. Cells were grown at 37 °C in 5% CO_2. For routine culture, cells were counted and plated at 2×10^5 cells per 75-cm^2 flask. Attachment efficiency was determined by counting attached cells 15 h after plating. The number of accumulated populations doublings (PD) per passage was determined using the equation, $PD = \log[A/(BC)]/\log 2$, where A is the number of collected cells, B is the number of plated cells, and C is the attachment efficiency.

Chromosomal analysis

Metaphase spreads were prepared from cells treated with Colcemid (KaryoMAX, GibcoBRL, 100 ng ml^{-1} for 6 h). We performed standard G-banding karyotypic analysis on at least 50 metaphase spreads for each population. Metaphase spreads were classified as abnormal if they contained any complement of chromosomes besides 46 XX with normal banding patterns.

Cell-cycle analysis

Cells were plated at an initial density of 5×10^4 cells per 25-cm^2 flask. Cells were

metabolically labelled with BrdU (10 μM, 4 h), trypsinized, and fixed with 70% ethanol. Nuclei were isolated and stained with propidium iodide and FITC-conjugated anti-BrdU antibodies (Becton Dickinson, USA), as described[7]. Flow cytometry was performed on a FACS Sorter (Becton Dickinson). All analysed events were gated to remove debris and aggregates.

Cell death assays

TUNEL assay for DNA fragmentation was done using an In Situ Cell Death Detection kit (BMB), according to manufacturer's protocol. Alternatively, cells were stained with Annexin-V-FLUOR (BMB) and propidium iodide, and analysed by fluorescence microscopy.

Telomere length assay

Genomic DNA (10 μg), isolated from cultured cells, was digested with restriction enzymes *Rsa*I and *Hin*fI and then separated in a 0.5% agarose gel. DNA was transferred to Hybond-N^+ membrane (Amersham, UK). Blots were probed with 5′-end-labelled oligonucleotide $(TTAGGG)_6$ and exposed to a PhosphoImager plate to detect the telomeric ends. An average telomere length was determined using ImageQuant software (Molecular Dynamics, USA).

Quantitative *in situ* hybridization with telomeric probe

In situ hybridization of telomere-specific peptide nucleic acid probe (Telomere PNA FISH Kit/Cy3, DAKO) to metaphase chromosome spreads was performed according to the manufacturer's protocol. Images were captured by a CCD camera attached to a Nikon TE300 microscope and analysed using IPLab Spectrum (Scanalytics Inc.). Background was subtracted and fluorescence signal was integrated in segments corresponding to individual telomeres[15].

Senescence-associated β-galactosidase assay

Senescence-associated β-galactosidase was detected in fixed cells using a described protocol[10]. When staining was fully developed, the cells were washed with PBS and incubated with propidium iodide (1 $\mu g\,ml^{-1}$ in PBS) and with DNase-free RNase A (5 $\mu g\,ml^{-1}$). Both phase-contrast and fluorescent microscopy were performed to identify senescent cells and their nuclei.

Western analysis

Whole-cell extracts were fractionated in gradient (4–20%) polyacrylamide gels (FMC) and transferred to Hybond-P (Amersham) membrane. The following antibodies were used: mouse monoclonal anti-human $p16^{ink4a}$(NeoMarkers, AB-1), mouse anti-p53 (Santa Cruz, DO-1), mouse anti-p21(WAF1) (Calbiochem, Ab-1), rabbit anti-$p14^{ARF}$ (NeoMarkers, Ab-1) and mouse anti-α-actin (Sigma); HRP-conjugated goat-anti-mouse antibody (GibcoBRL) and goat anti-rabbit antibody (Calbiochem). Staining was developed using ECL-detection protocol.

Received 21 September; accepted 16 November 2000.

1. Shay, J. W., Wright, W. E. & Werbin, H. Toward a molecular understanding of human breast cancer: a hypothesis. *Breast Cancer Res. Treatment.* **25** 83–94 (1993).
2. Hayflick, L. The limited *in vitro* lifetime of human diploid cell strains. *Exp. Cell Res.* **37,** 614–636 (1965).
3. Hammond, S. L., Ham, R. G. & Stampfer, M. R. Serum-free growth of human mammary epithelial cells: rapid clonal growth in defined medium and extended passage with pituitary extract. *Proc. Natl Acad. Sci. USA* **81,** 5435–5439 (1984).
4. Foster, S. A. & Galloway, D. A. Human papillomavirus type 16 E7 alleviates a proliferation block in early passage human mammary epithelial cells. *Oncogene* **12,** 1773–1779 (1996).
5. Huschtscha, L. I. *et al.* Loss of $p16^{INK4}$ expression by methylation is associated with lifespan extension of human mammary epithelial cells. *Cancer Res.* **58,** 3508–3512 (1998).
6. Kiyono, T. *et al.* Both Rb/$p16^{INK4a}$ inactivation and telomerase activity are required to immortalize human epithelial cells. *Nature* **396,** 84–88 (1998).
7. Meyer, K. M., Hess, S. M., Tlsty, T. D. & Leadon, S. A. Human mammary epithelial cells exhibit a differential p53-mediated response following exposure to ionizing or UV light. *Oncogene* **18,** 5792–57805 (1999).
8. Walen, K. H. & Stampfer, M. R. Chromosome analyses of human mammary epithelial cells at stages of chemical-induced transformation progression to immortality. *Cancer Genet. Cytogenet.* **37,** 249–261 (1989).
9. Brenner, A. J., Stampfer, M. R. & Aldaz, C. M. Increased p16 expression with first senescence arrest in human mammary epithelial cells and extended growth capacity with p16 inactivation. *Oncogene* **17,** 199–205 (1998).
10. Dimri, G. P. *et al.* A biomarker that identifies senescent human cells in culture and in aging skin *in vivo*. *Proc. Natl Acad. Sci. USA* **92,** 9363–9367 (1995).
11. Pignolo, R. J., Rotenberg, M. O. & Cristofalo, V. J. Alterations in contact and density-dependent arrest state in senescent WI-38 cells. *In Vitro Cell. Dev. Biol. Anim.* **30A,** 471–476 (1994).
12. Shay, J. W. & Wright, W. E. Quantitation of the frequency of immortalization of normal human diploid fibroblasts by SV40 large T-antigen. *Exp. Cell Res.* **184,** 109–118 (1989).
13. Taylor-Papadimitriou, J. *et al.* Keratin expression in human mammary epithelial cells cultured from normal and malignant tissue: relation to *in vivo* phenotypes and influence of medium. *J. Cell Sci.* **94,** 403–413 (1989).
14. Foster, S. A., Wong, D. J., Barrett, M. T. & Galloway, D. A. Inactivation of p16 in human mammary epithelial cells by CpG island methylation. *Mol. Cell. Biol.* **18,** 1793–1801 (1998).
15. Lansdorp, P. M. *et al.* Heterogeneity in telomere length of human chromosomes. *Hum. Mol. Genet.* **5,** 685–691 (1996).
16. van Steensel, B., Smogorzewska, A. & de Lange, T. TRF2 protects human telomeres from end-to-end fusions. *Cell* **92,** 401–413 (1998).
17. Stampfer, M. R. *et al.* Gradual phenotypic conversion associated with immortalization of cultured human mammary epithelial cells. *Mol. Biol. Cell* **8,** 2391–2405 (1997).
18. Karlseder, J., Broccoli, D., Dai, Y., Hardy, S. & de Lange, T. p53- and ATM-dependent apoptosis induced by telomeres lacking TRF2. *Science* **283,** 1321–1325 (1999).
19. Artandi, S. E. *et al.* Telomere dysfunction promotes non-reciprocal translocations and epithelial cancers in mice. *Nature* **406,** 641–645 (2000).
20. Chin, L. *et al.* p53 Deficiency rescues the adverse effects of telomere loss and cooperates with telomere dysfunction to accelerate carcinogenesis. *Cell* **97,** 527–538 (1999).
21. Alcorta, D. A. *et al.* Involvement of the cyclin-dependent kinase inhibitor p16 (INK4A) in replicative senescence of normal human fibroblasts. *Proc. Natl Acad. Sci. USA* **92,** 13742–13747 (1996).
22. Hara, E. *et al.* Regulation of p16CDKN2 expression and its implications for cell immortalization and senescence. *Mol. Cell. Biol.* **16,** 859–867 (1996).
23. Burbano, R. R. *et al.* Cytogenetics of epithelial hyperplasias of the human breast. *Cancer Genet. Cytogenet.* **119,** 62–66 (2000).
24. Pandis, N. *et al.* Chromosome abnormalities in bilateral breast carcinomas. Cytogenetic evaluation of the clonal origin of multiple primary tumors. *Cancer* **76,** 250–258 (1995).
25. Berg, J. W. & Hutter, R. V. Breast cancer. *Cancer* **75,** 257–269 (1995).
26. Stoeber, K. *et al.* Cdc6 protein causes premature entry into S phase in a mammalian cell-free system. *EMBO J.* **17,** 7219–7229 (1998).
27. Wei, W. & Sedivy, J. M. Differentiation between senescence (M1) and crisis (M2) in human fibroblasts cultures. *Exp. Cell Res.* **253,** 519–522 (1999).
28. Tlsty, T. D. *et al.* Potentiation of genomic instability in normal human mammary epithelial cells by an epigenetic event. *J. Mammary Gland Biol. Neoplasia* (in the press).

Supplementary information is available on *Nature*'s World-Wide Web site (http://www.nature.com) or as paper copy from the London editorial office of *Nature*.

Acknowledgements

We thank E. H. Blackburn, I. Herskowitz and J. Li for comments, criticism and reading the manuscript. Stimulating discussion and thoughtful critique were provided by Y. Crawford, G. Whitworth, M. Heiman, M. Springer, D. Crawford, P. Hein and J. Anderson. We thank S. Gilbert for assistance with the figures; P. Ortiz for library support; and G. Williams for MCM2 antibodies. This work was supported by NIH and NIH/NASA grants to T.D.T. and a DOE and NIH grant to M.R.S. C.R.H. is supported by a Howard Hughes Pre-doctoral Fellowship.

Correspondence and requests for materials should be addressed to T.D.T. (e=mail: ttlsty@itsa.ucsf.edu).

The bacterial conjugation protein TrwB resembles ring helicases and F_1-ATPase

F. Xavier Gomis-Rüth*, Gabriel Moncalián†, Rosa Pérez-Luque*, Ana González‡§, Elena Cabezón†, Fernando de la Cruz† & Miquel Coll*

** Institut de Biologia Molecular de Barcelona, CSIC, Jordi Girona, 18-26, 08034 Barcelona, Spain*
† Departamento de Biología Molecular (Laboratorio asociado al CIB, CSIC), Universidad de Cantabria, Herrera Oria, 39011 Santander, Spain
‡ EMBL Hamburg Outstation, c/o DESY, Notkestrasse 85, 22603 Hamburg, Germany

The transfer of DNA across membranes and between cells is a central biological process; however, its molecular mechanism remains unknown. In prokaryotes, *trans*-membrane passage by bacterial conjugation, is the main route for horizontal gene transfer. It is the means for rapid acquisition of new genetic information, including antibiotic resistance by pathogens. *Trans*-kingdom gene transfer from bacteria to plants[1] or fungi[2] and even bacterial sporulation[3] are special cases of conjugation. An integral membrane DNA-binding protein, called TrwB in the *Escherichia coli* R388 conjugative system, is essential for the conjugation process. This large multimeric protein is responsible for recruiting the relaxosome DNA–protein complex, and participates in the

§ Present address: Stanford Linear Accelerator Center, 2575 Sand Hill Road, Mail Stop 99, Menlo Park, California 94025, USA.